THE VIBRATIONS OF BUBBLES AND BALLOONS

Kirsty A. Kuo and Hugh E.M. Hunt
Faculty of Engineering, University of Cambridge, Trumpington St., Cambridge CB2 1PZ, UK
kan26@cam.ac.uk

Bubbles and balloons are two examples of structures that feature a pressure difference across the skin, a thin, tensioned membrane, and a doubly curved interface surface. While mathematical models have been formulated for bubble vibrations, no such model exists for balloon vibrations. This paper reviews a model of bubble vibrations, and compares its predicted natural frequencies and modeshapes to those of a rubber balloon. It is shown that the bubble model consistently underpredicts the balloon's natural frequencies, and it is concluded that the nonlinear elasticity present in the balloon skin accounts for this result.

INTRODUCTION

There are many examples of thin-walled, inflated shells in our lives – think of airbags, basketballs, tyres, eyeballs, soap bubbles and balloons. These objects may be toroidal, spherical, or some more generalised ovoidal shape, but they all have three features in common: a pressure difference across the skin; a thin, tensioned membrane; and a doubly curved interface surface. This means that for all of these systems, a common set of fundamental equations of motion will form the basis of a derivation of the vibration modes. Hence, once an analytical solution to the vibration of one of these systems (e.g. soap bubbles) has been obtained, theory can be extrapolated to aid in describing another of these systems (e.g. balloons). This is the approach taken in this paper to investigate the vibrations of balloons.

The wider context of this research is the dynamic modelling of high-altitude tethered balloons, which have attracted interest recently due to their potential uses in mobile communications, meteorology, energy harvesting and climate engineering. Recent papers on the dynamics of high-altitude tethered balloons [1-4] treat the balloon as a rigid body. The spherical or streamlined shape of the balloon affects the lift and drag forces, but it is assumed that the forcing from the tether does not result in balloon deformations. However, when the authors observed a 1m-diameter meteorological balloon tethered at 15m, a strong vibration coupling between axial excitation of the tether and ovalling deformations of the balloon was seen. This suggests that higher-order modes can be excited on tethered balloons.

In this paper, the balloon is assumed to have a spherical shape. This is the simplest balloon shape, and is a good approximation to the shape of meteorological balloons and small-scale high-altitude balloons. Streamlined aerostats that exhibit weather-vaning behaviour, and the pumpkin-shaped envelopes that are designed to reduce hoop stresses in large high-altitude balloons are considered beyond the scope of this paper.

A literature search on balloon vibrations revealed that no mathematical model had been specifically derived for balloons, so our attention turned to other inflated shells. Analogous studies of the vibration modes of thin-walled spherical shells were found, including those with application to inflatable cushions [5], pneumatic tires [6], eyeballs [7], heart ventricles [8], soap bubbles [9-10] and basketballs [11]. These studies use a combination of one or more of analytical techniques, finite element analysis and experimental measurement to determine modeshapes and natural frequencies. Of all the inflated shells that were identified, soap bubbles had received the most attention in the modelling literature, and as they are of a similar spherical geometry to balloons, bubbles were chosen as the closest analogue for the purpose of studying the vibration modes and natural frequencies.

This paper describes a model of soap bubble vibrations, and compares the results of this model to the experimentally measured response of a rubber balloon. The calculated natural frequencies and modeshapes are compared, and conclusions regarding the suitability of this predictive model are made.

BUBBLE VIBRATIONS

The earliest analysis of the bubble vibration problem was performed by Rayleigh [12], in his study of the vibration of a liquid mass about a spherical figure. This analysis was extended by Lamb in 1895, in his book *Hydrodynamics* [13], to account for the surrounding fluid. Lamb's well-known solution describes a spherical bubble of one fluid (e.g. air) immersed within a second fluid (e.g. water), which is often described as a 'droplet'. Lamb begins by assuming an expression for the shape of the common surface, and then uses it to find the corresponding velocity potential and pressure at internal and external points. Using the Theorem for Solid Geometry and the expression for surface tension, he derives this closed-form solution for the natural frequencies ω_j of the bubble

$$\omega_j{}^2 = \frac{\sigma}{R^3} \frac{(j\text{-}1)j(j+1)(j+2)}{(j+1)\rho^+ + j\rho^-} \tag{1}$$

where σ is the surface tension, R is the radius, j is the mode number ($j = 1, 2, ...$), ρ^+ is the fluid density inside the droplet, and ρ^- is the fluid density outside the droplet. (For an explanation of why $j \neq 0$, refer to the Comparison of Results section).

It was more than one hundred years later that a solution to the vibration of soap bubbles was formulated by Grinfeld [10]. Grinfeld's model includes the inertia of the bubble film,

thus representing a system that comprises three different fluids: the inner fluid, the film fluid, and the outer fluid. To derive this model, Grinfeld begins with the linearised form of Euler's equations governing inviscid flow

$$\frac{\partial v^i}{\partial t} = -\frac{1}{\rho} \nabla^i p \tag{2a}$$

$$\nabla_i v^i = 0 \tag{2b}$$

where v^i is the covariant component of the velocity fields, ρ is the surrounding fluid density (either ρ^+ or ρ^- depending on the domain) and p is the pressure. The momentum and velocity components in each of the three spherical coordinate directions are derived, and the condition that the ambient velocity field in the radial direction must be equal on either side of the bubble film is applied.

The equations for the dynamic behaviour of the bubble film are formulated using a Laplace capillarity model, and include interaction with the ambient air. The detailed formulation of these equations can be found in [14, 15]. For a fluid film with constant thickness, the linearised equation is

$$\tau_0 \frac{\partial^2 c}{\partial t^2} = \sigma \left(\nabla_\alpha \nabla^\alpha c + \frac{2}{R^2} c \right) + \left[\frac{\partial p}{\partial t} \right] \tag{3}$$

where τ_0 is the uniform equilibrium two-dimensional mass density of the film, c is the small component of the velocity field, $\nabla_\alpha \nabla^\alpha$ is the surface Laplacian, and the symbol $[p]$ denotes the jump in ambient pressure across the surface of the film.

Equations (2a), (2b) and (3) combine to give a dispersion relationship, which is solved to obtain the natural frequencies of the soap bubble

$$\omega_j^2 = \frac{\sigma}{R^3} \frac{(j-1)j(j+1)(j+2)}{j(j+1)\tau_0 R^{-1} + (j+1)\rho^+ + j\rho^-} \tag{4}$$

As the mass density of the film approaches zero, this equation is shown to reduce to Lamb's 'droplet' solution.

The modeshapes that correspond to these natural frequencies are proportional to the surface spherical harmonics, $Y_{jn}(\theta,\varphi)$, where the mathematical convention for spherical coordinates is adopted such that θ is the azimuthal angle, and φ is the polar angle. In orthonormal form, the surface spherical harmonics are made up of the following two expressions

$$\sqrt{\frac{2j+1}{2\pi} \frac{(j-n)!}{(j+n)!}} P_j^n(\cos \varphi) \cos n\theta \tag{5a}$$

$$\sqrt{\frac{2j+1}{2\pi} \frac{(j-n)!}{(j+n)!}} P_j^n(\cos \varphi) \sin n\theta \tag{5b}$$

where $P_j^n(\cos \varphi)$ are associated Legendre functions of the first kind of degree j and order n. The modeshapes for $j = 0,1,2,3$ are illustrated in Figure 1, where the colouring indicates the amount of deflection in the radial direction. The modeshape corresponding to $j = 0$ is called the 'breathing mode', as it involves uniform radial extension over the entire sphere. The modeshapes corresponding to $j = 1$ represent the three orthogonal rigid-body modes.

To obtain the frequency-response function from the natural frequencies and mode shapes of the bubble, the general equation from Newland [16] can be used. The frequency-response function $H(\mathbf{z}_r, \mathbf{z}_s, \omega)$ of an undamped system, with output measured at location $\mathbf{z}_r$ and subjected to a unit harmonic input force at location $\mathbf{z}_s$ is given in Newland [16] as

$$H(\mathbf{z}_r, \mathbf{z}_s, \omega) = \Sigma_{j=0}^\infty \frac{U_j(\mathbf{z}_r)U_j(\mathbf{z}_s)}{\omega_j^2 - \omega^2} \tag{6}$$

where $U_j(\mathbf{z}_r)$ is the mass-normalised mode function of mode j, evaluated at $\mathbf{z}_r$. For the case of the vibrating bubble skin, the mass-normalised mode function is represented solely by the contribution of the membrane displacement in the radial direction, that is, the surface spherical harmonics. The mass-normalisation condition is expressed as

$$\lambda^2 \int_0^{2\pi} \int_0^\pi Y_{jn}(\theta,\varphi) \, \tau_0 R^2 d\varphi d\theta = 1 \tag{7}$$

where λ is the normalisation constant. The normalisation constant is found by numerically evaluating Eq. (7) in the modelling program. For comparison with the experimental results in the next section, the driving-point response of the bubble is to be evaluated at the south pole, that is, at $\mathbf{z}_r = \mathbf{z}_s = (a, 0, \pi)$. This means that only the axisymmetric modeshapes ($n = 0$) are excited, hence the response of the bubble is given by

$$H(\mathbf{z}_r, \mathbf{z}_s, \omega) = \Sigma_{j=0}^\infty \frac{\lambda^2 Y_{j0}(0,\pi)Y_{j0}(0,\pi)}{\omega_j^2 - \omega^2} \tag{8}$$

Having determined the frequency-response function for the vibrations of soap bubbles, we now turn out attention to the vibrations of balloons.

$j=0, n=0$

$j=1, n=0$ $j=1, n=1$ $j=1, n=1$

$j=2, n=0$ $j=2, n=1$ $j=2, n=1$ $j=2, n=2$ $j=2, n=2$

$j=3, n=0$ $j=3, n=1$ $j=3, n=1$ $j=3, n=2$ $j=3, n=2$ $j=3, n=3$ $j=3, n=3$
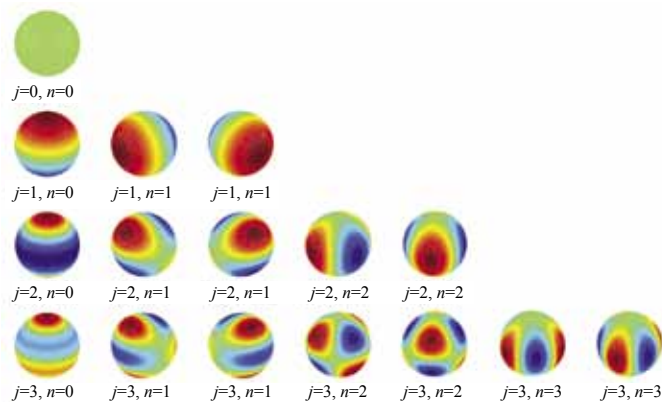
Figure 1. The spherical surface harmonics for $j = 0,1,2,3$

BALLOON VIBRATIONS

There is no mathematical model for balloon vibrations in the literature, hence we embarked on a series of experiments to determine the natural frequencies and modeshapes of a large, spherical, helium-filled novelty balloon.

The natural frequencies were determined by measuring the driving-point frequency-response function of the balloon, using an impact hammer and a laser vibrometer. The impact hammer

was used to deliver an impulse to the base of the balloon, near the neck, and the laser beam was aimed at a piece of reflective tape positioned as close as possible to the impact point. The data from the impact hammer and the laser vibrometer were logged and analysed using a customised Matlab program. The experimental setup is shown in Fig. 2.
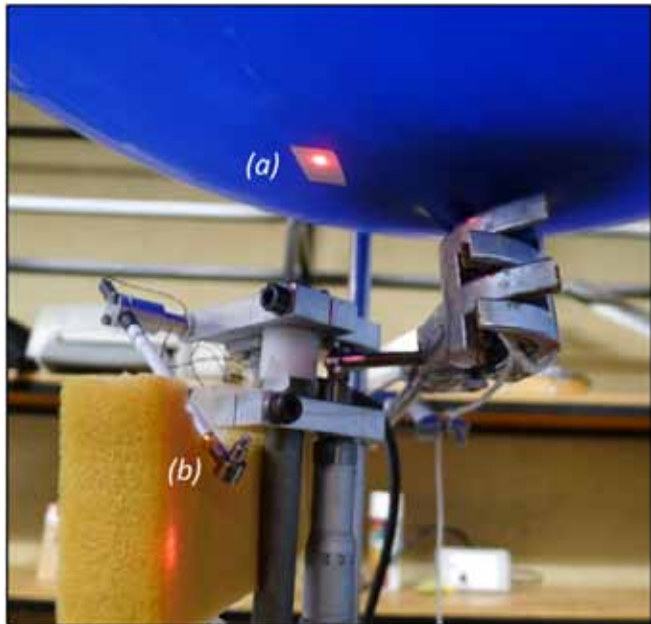
Figure 2. The experimental setup used to measure the balloon vibration modes, showing (a) the laser beam from the vibrometer, aimed at a piece of reflective tape near the base of the balloon; and (b) the impact hammer used to deliver an impulse to the base of the balloon.

The balloon is made of rubber latex, and has a design diameter of 1m, though was only partially inflated for ease of handling. The laser vibrometer is a Polytec OFV302 single-point vibrometer, connected through a Polytec OFV 3001 vibrometer controller. The velocity range is 1000mm/s/V and the velocity filter is set at 2.4kHz. The impact hammer is a miniature instrumented impact hammer, model PCB 086E80. The experimental parameters for this balloon are given in Table 1. The pressure in the balloon was measured by connecting the balloon to a U-tube manometer.

The balloon is very sensitive to disturbances in the surrounding air, and to minimise movement of the balloon it was restrained by a clamp on the neck, below the tie-off point. A total of 50 hammer impacts were used to calculate an averaged velocity frequency-response function. The major peaks of this frequency-response function represent the natural frequencies of the balloon, and the first eight peaks occur at 0.63Hz, 6.8Hz, 55.1Hz, 79.8Hz, 105Hz, 131Hz, 157Hz, and 185Hz. The coherence lies between 0.9 and 1.0 over the measured frequency range of 0Hz to 300Hz, hence the resonant behaviour of the balloon in this range is due to the hammer impact. Figure 3 shows the measured velocity frequency-response function of the balloon, as a function of frequency.

Also overlaid on Fig. 3 is the driving-point response

calculated using the mathematical model of the soap bubble, with the experimental parameters given in Table 1 being used as the input to this model. The surface tension for the soap bubble model is calculated by equating the outwards-acting force due to the internal pressure with the restoring force provided by the surface tension, such that

$$\sigma = \frac{pR}{2} \tag{9}$$

(Note that the surface tension in the soap bubble model is a factor of two larger than the surface tension acting in a droplet, as the bubble has two film surfaces as opposed to the one surface that separates the fluids in a droplet). The two-dimensional mass density of the film τ_0 is calculated as the balloon skin mass divided by the surface area of the balloon, $4\pi R^2$. The densities of the helium inside the balloon ρ^+ and the air outside the balloon ρ^- are calculated using the measured pressures and temperature, and the perfect gas law.

Table 1. Experimental parameters

Parameter	Value
Balloon radius	0.32m
Balloon skin mass	3.5×10^{-2}kg
Internal pressure (gauge)	1.27×10^{3}Pa
Atmospheric pressure	1.03×10^{5}Pa
Atmospheric temperature	291K
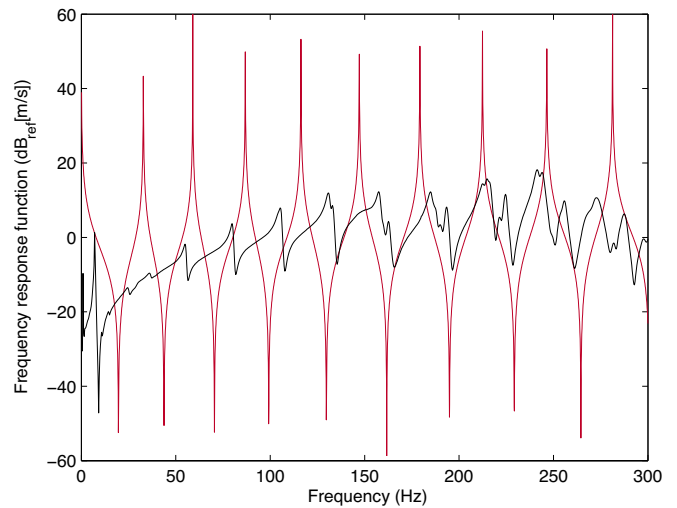
Figure 3. The experimentally measured driving-point response of the balloon is shown in black, and the red line shows the driving-point response predicted using the soap-bubble model, with the balloon parameters as inputs.

COMPARISON OF RESULTS

There are obvious differences between the experimentally measured response of the balloon and the response predicted using the soap-bubble model, and in this section we look at why these differences occur.

For both balloons and soap bubbles, it is reasonable to assume that the gas inside the balloon is incompressible, hence the volume of the sphere is constant and the $j = 0$ breathing mode at 0Hz is not expected to occur. This is consistent with the experimental observations, as no peak at 0Hz is observed.

The first peak in the experimental results occurs at 0.63Hz, and visual observation of the balloon indicates that this peak corresponds to a low-frequency, lightly damped, rigid-body rocking motion of the balloon about the clamp. The balloon was highly sensitive to air-flow disturbances caused by nearby movements, making it particularly difficult to avoid excitation of this mode. As the bottom restraint of the balloon is not included in the soap-bubble model, there is no equivalent natural frequency seen in the predictions of the mathematical model.

The second peak in the experimental results occurs at 6.8Hz, and visual observation of the balloon indicates that this peak corresponds to the theoretical $j = 1$ mode: vertical rigid-body translation of the balloon's centre of mass. Although the soap-bubble model predicts that this occurs at 0Hz, the peak has been shifted slightly. This is because the balloon's neck and the low-tension material at the base of the balloon are acting together as a 'spring' that separates the balloon from the clamp.

To investigate the modeshapes that occur at higher frequencies, the balloon was excited acoustically using an amplifier and speaker system at a pure tone that matched each of the natural frequencies. Visual and tactile observation of the balloon's vibrations indicated that the 55.1Hz mode has two latitudinal nodal lines, arranged identically to the $j = 2$, $n = 0$ modeshape shown in Figure 1. This suggests that the natural frequency at 55.1Hz is due to the $j = 2$ modeshape. The number of latitudinal nodal lines was observed to increase linearly as the pure tone was matched to the higher natural frequencies: three nodal lines at 79.8Hz ($j = 3$, $n = 0$), four at 105Hz ($j = 4$, $n = 0$), and five at 131Hz ($j = 5$, $n = 0$).

There is a discrepancy between the modelling predictions and the experimental results at these higher frequencies, with the mathematical model consistently underpredicting the natural frequencies of the balloon. The reason for this is believed to be elasticity which is present in the balloon skin, but not accounted for in the bubble model. Grinfeld's bubble model assumes that the bubble film is inelastic, as fluids have a constant value of surface tension, and thus there is no capacity for elastic energy to be stored in the skin during inflation or bubble deformation. The balloon, however, is made of a viscoelastic material that stretches as it inflates and undergoes changes in geometry.

The effect of skin elasticity on the natural frequencies can be evaluated using energy methods. Rayleigh's quotient is a means of approximating natural frequencies, and is based on equating the kinetic and potential energy of vibration, assuming negligible energy loss per cycle, that is, a lightly damped system [17]. The skin elasticity can be incorporated into Rayleigh's quotient by the addition of an extra potential energy term in the numerator. (Note that this extra potential energy term is only relevant for those modes that involve deformation from the spherical 'equilibrium' geometry, and thus only occur for $j \geq 2$). This additional term results in an increase in the natural frequencies, thus predicting that the natural frequencies of the elastic balloon will be greater than those of a soap bubble with constant surface tension when $j \geq 2$. This is consistent with the results presented here.

It can be seen in Fig. 3 that as the frequency increases, the major peaks in the balloon's driving point response begin to separate into clusters of closely-spaced peaks. This separation is due to the inhomogeneity of the balloon, which has a more pronounced effect on higher frequencies as the modal displacement variation occurs over shorter distances. Inhomogeneity exists in the shape of the balloon, the thickness of the balloon skin, and the surface tension in the balloon skin.

CONCLUSIONS

Bubbles have been well-studied in fluid-mechanics literature, and a mathematical model exists for predicting their natural frequencies and modeshapes. These natural frequencies depend on fluid properties and geometry, and the modeshapes correspond to the spherical surface harmonics. There is no mathematical model for balloon vibrations in the literature, and this paper has shown that the bubble model consistently underpredicts the natural frequencies observed for a balloon. This underprediction is due to the elasticity that is present in the balloon skin, but neglected from the bubble model. Work is currently underway to formulate an analytical solution for the natural frequencies of a spherical, elastic membrane with internal and external fluid interactions.

ACKNOWLEDGEMENTS

REFERENCES

[1] G.S. Aglietti, "Dynamic response of a high-altitude tethered balloon system", *Journal of Aircraft* **46**(6), 2032-2040 (2009)

[2] K.A. Stanney and C.D. Rahn, "Response of a tethered aerostat to simulated turbulence", *Communications in Nonlinear Science and Numerical Simulation* **11**, 759-776 (2006)

[3] C. Lambert and M. Nahon, "Stability analysis of a tethered aerostat", *Journal of Aircraft* **40**(4), 705-715 (2003)

[4] P. Coulombe-Pontbriand and M. Nahon, "Experimental testing and modelling of a tethered spherical aerostat in an outdoor environment", *Journal of Wind Engineering and Industrial Aerodynamics* **97**, 208-218 (2009)

[5] L.E. Penzes and H. Kraus, "Free vibration of an inflated oblate spheroidal shell", *Journal of Sound and Vibration* **27**(4), 559-572 (1973)

[6] L.E. Kung, W. Soedel and T.Y. Yang, "Free vibration of a pneumatic tire-wheel unit using a ring on an elastic foundation and a finite element model", *Journal of Sound and Vibration* **107**(2), 181-194 (1986)

[7] L. Coquart, C. Depeursinge, A. Curnier and R. Ohayon, "A fluid-structure interaction problem in biomechanics: prestressed vibrations of the eye by the finite element method", *Journal of Biomechanics* **25**(10), 1105-1118 (1992)

[8] A. Singer, "Computed ventricular acoustic frequency", *Bulletin of Mathematical Biophysics* **29**, 465-471 (1967)

[9] G. Rämme, "Modelling the atom by rotating and vibrating soap bubbles", *Physics Education* **29**, 313-318 (1994)

[10] P. Grinfeld, "Small oscillations of a soap bubble", *Studies in Applied Mathematics* **128**(1), 30-39 (2012)

[11] D. Russell, "Basketballs as spherical acoustic cavities", *American Journal of Physics* **78**(6), 549-554 (2010)

[12] L. Rayleigh, "On the capillary phenomena of jets", *Proceedings of the Royal Society of London (1854-1905)* **29**(10), 71-97 (1879)

[13] H. Lamb, *Hydrodynamics*, Dover Publications, New York, 1993

[14] P. Grinfeld, "Exact nonlinear equations for fluid films and proper adaptations of conservation theorems from classical hydrodynamics", *Journal of Geometry and Symmetry in Physics* **16**, 1-21 (2009)

[15] P. Grinfeld, "Hamiltonian dynamic equations for fluid films", *Studies in Applied Mathematics* **125**, 223-264 (2010)

[16] D.E. Newland, *Mechanical Vibration Analysis and Computation*, Dover Publications, Inc. Mineola, 1989

THEME

ACOUSTICS 2013, the annual conference of the Australian Acoustical Society, will be held in Victor Harbor, South Australia, at the McCracken Country Club, from 17-19 November 2013.

With its theme of Science, Technology and Amenity, Acoustics 2013 Victor Harbor will include plenary sessions addressing the impact of science and technology on acoustics and amenity, whether it be environmental or internal spaces. Other major streams will address airport / road / railway noise, standards and guidelines including those from EPAs, underwater acoustics, marine bioacoustics and vibration.

Acoustics 2013 Victor Harbor will provide in-depth coverage of many topics of interest to professionals in related fields including educationalists, consultants, planners, developers, government authorities, and EPA/noise officers

VENUE

Acoustics 2013 Victor Harbor will be held at the McCracken Country Club. The 4.5 star McCracken Country Club offers guests luxurious accommodation in the beachside township of Victor Harbor. The country club highlights are its golf course, day spa and the gorgeous panoramic view of Hindmarsh Valley. Visit www.countryclubs.com.au/mccracken/

TOPICS

In addition to the main conference themes, Acoustics 2013 Victor Harbor will include sessions on:
- Environmental acoustics
- Industrial acoustics
- Wind turbine noise
- Low frequency noise
- Internal spaces and amenity
- Architectural acoustics
- Underwater acoustics
- Marine bioacoustics
- Legislation and standards
- Transportation noise

WORKSHOPS

A series of workshops are planned. The following workshop will be held:
- Flow induced noise

For up-to-date information regarding the Acoustics 2013 Victor Harbor conference, please visit the conference website: www.acoustics.asn.au/joomla/acoustics-2013.html